American Physiological Society | AMERICAN JOURNAL OF PHYSIOLOGY Endocrinology and Metabolism
PUBLISHED ARTICLE ARCHIVES SUBSCRIPTIONS SUBMISSIONS CONTACT US

Am J Physiol Endocrinol Metab. 2018 Oct 1; 315(4): E594–E604.
Published online 2018 Feb 20.
doi: 10.1152/ajpendo.00343.2017: 10.1152/ajpendo.00343.2017

PMCID: PMC6230710
PMID: 29558205

Fibroblast growth factor 23 does not directly influence skeletal muscle cell proliferation and differentiation or ex vivo muscle contractility

Keith G. Avin,[1,2,*] Julian A. Vallejo,[3,4,*] Neal X. Chen,[2] Kun Wang,[4] Chad D. Touchberry,[3] Marco Brotto,[5] Sarah L. Dallas,[4] Sharon M. Moe,[2,6] and Michael J. Wacker[3]

[1]Department of Physical Therapy, School of Health and Rehabilitation Sciences, Indiana University, Indianapolis, Indiana
[2]Division of Nephrology, Department of Medicine, Indiana University School of Medicine, Indianapolis, Indiana
[3]Department of Biomedical Sciences, School of Medicine, University of Missouri-Kansas City, Kansas City, Missouri
[4]Department of Oral and Craniofacial Sciences, School of Dentistry, University of Missouri-Kansas City, Kansas City, Missouri
[5]College of Nursing and Health Innovation, Bone-Muscle Collaborative Sciences, University of Texas-Arlington, Arlington, Texas
[6]Roudebush Veterans Administration Medical Center, Indianapolis, Indiana
Corresponding author.
[*]K. G. Avin and J. A. Vallejo contributed equally to this work.
Address for reprint requests and other correspondence: M. J. Wacker, 2411 Holmes St., Dept. of Biomedical Sciences, UMKC School of Medicine, Kansas City, MO 64108 (e-mail: wackerm@umkc.edu).

Received 2017 Sep 25; Revised 2018 Jan 29; Accepted 2018 Feb 15.

Abstract

Skeletal muscle dysfunction accompanies the clinical disorders of chronic kidney disease (CKD) and hereditary hypophosphatemic rickets. In both disorders, fibroblast growth factor 23 (FGF23), a bone-derived hormone regulating phosphate and vitamin D metabolism, becomes chronically elevated. FGF23 has been shown to play a direct role in cardiac muscle dysfunction; however, it is unknown whether FGF23 potential FGF23 receptors (*Fgfr1–4*) and *α-Klotho* in muscles of two animal models (CD-1 and Cy/+ rat, a naturally occurring rat model of chronic kidney disease-mineral bone disorder) as well as C_2C_{12} myoblasts and myotubes. C_2C_{12} proliferation, myogenic gene expression, oxidative stress marker 8-OHdG, intracellular Ca^{2+} ($[Ca^{2+}]_i$), and ex vivo contractility of extensor digitorum longus (EDL) or soleus muscles were assessed after treatment with various amounts of FGF23. FGF23 (2–100 ng/ml) did not alter C_2C_{12} proliferation, expression of myogenic genes, or oxidative stress after 24- to 72-h treatment. Acute or prolonged FGF23 treatment up to 6 days did not alter C_2C_{12} $[Ca^{2+}]_i$ handling, nor did acute treatment with FGF23 (9–100 ng/ml) affect EDL and soleus muscle contractility. In conclusion, although skeletal muscles express the receptors involved in FGF23-mediated signaling, in vitro FGF23 treatments failed to directly alter skeletal muscle development or function under the conditions tested. We hypothesize that other endogenous substances may be required to act in concert with FGF23 or apart from FGF23 to promote

muscle dysfunction in hereditary hypophosphatemic rickets and CKD.

Keywords: chronic kidney disease, fibroblast growth factor 23, hypophosphatemic rickets, intracellular Ca^{2+}, myogenesis

INTRODUCTION

FGF23 is a bone-derived hormone that controls phosphate and 1,25-dihydroxyvitamin D [$1,25(OH)_2D$] metabolism by suppressing renal phosphate reabsorption and $1,25(OH)_2D$ synthesis (8). FGF23 signaling is dependent upon a number of factors, including the FGF receptors (FGFRs) (R1, R2, R3, or R4), potential involvement of α-Klotho coreceptor, and cell type (18, 28, 39, 42). Elevated serum FGF23 concentrations are associated with lower left ventricular ejection fraction (43) and cardiovascular disease across a number of patient populations, including end-stage renal disease and patients on hemodialysis (22). FGF23 has been shown to act directly on the heart by inducing pathological hypertrophy (14), whereas our group has shown that FGF23 also directly and acutely alters myocardial contractility and increases the amount of intracellular Ca^{2+} ($[Ca^{2+}]_i$) (52). Given the direct effects of FGF23 on cardiac muscle, there may be a relationship of FGF23 with skeletal muscle function as well.

FGF23 serum levels are significantly elevated in the clinical disorders of chronic kidney disease (CKD) and hereditary hypophosphatemic rickets, both of which result in skeletal muscle dysfunction (16, 53). Specifically, in patients with CKD and end-stage renal disease, FGF23 can be elevated up to 1,000-fold above normal levels (21, 26), and there are documented deficits of functional capacity and strength in the muscles of both patients and animals models with CKD and hemodialysis treatment (16, 23, 33).

In hereditary hypophosphatemic rickets, chronic accumulation of FGF23 in the serum is attributed to mutations in genes regulating FGF23 production and has been shown to be associated with muscle function abnormalities (53, 54). The murine homolog model of X-linked hypophosphatemic rickets (XLH), the *Hyp* mouse, shows reduced grip strength and low spontaneous motor activity (5). Patients with XLH who were treated with four monthly doses of a human monoclonal anti-FGF23 antibody reported significant improvements in patient perception of quality of life and muscle stiffness (40). Additionally, our group has shown that skeletal muscles of the *Dmp1*-null mouse, a model of autosomal recessive hypophosphatemic rickets (ARHR), display significant impairments in muscle-specific force production and $[Ca^{2+}]_i$ homeostasis (55). Despite some of these associations and studies, it remains unclear whether skeletal muscle development and functional properties may be directly altered by FGF23.

Therefore, in the present study, we sought to identify the direct role of FGF23 on skeletal muscle function by assessing markers of cellular proliferation, muscle fiber development, oxidative stress, and $[Ca^{2+}]_i$ handling properties in C_2C_{12} cells as well as functional parameters of isolated murine fast-twitch [extensor digitorum longus (EDL)] and slow-twitch (soleus) muscles after treatment with FGF23. Two laboratories independently collected data for this study, and the results are presented collectively in this article.

METHODS

Experiments performed. Laboratories at Indiana University carried out gene expression studies on a CKD rat model, proliferation of C_2C_{12} cells using CellTiter 96 AQueous One kit, myogenic gene expression markers, and oxidative stress marker and Rhod-3 Ca^{2+} measurements. The laboratory at the University of Missouri-Kansas City carried out gene expression analysis of CD-1 mouse EDL and soleus and C_2C_{12} cells, proliferation of C_2C_{12} by MTT and hemocytometer measurements, fluo-4 Ca^{2+} measurements, and ex vivo contractility of EDL, soleus, and heart.

Animal models. All procedures were reviewed and approved by the Indiana University School of Medicine and University of Missouri-Kansas City Institutional Animal Care and Use Committees, which

adhered to the *Guide for Care and Use of Laboratory Animals* to minimize pain and suffering. Two animal models were used in this study: *1*) CD-1 mice (Harlan Laboratories, Madison, WI) and *2*) the Cy/+ rat model of chronic kidney disease-mineral bone disorder (CKD rat). The Cy/+ rat model is an autosomal-dominant, slow progressing model of CKD due to a missense mutation in the gene *Anks6* that results in terminal uremia by 40 wk and development of chronic kidney disease-mineral bone disorder (CKD-MBD) (30).

Male virgin CD-1 mice were euthanized at 3–5 mo of age by cervical dislocation for harvesting of EDL and soleus muscles for RNA isolation and contractility analysis. Male CKD rats and normal littermates were housed as previously described (6) and euthanized at 8 mo with pentobarbital sodium (50 mg/kg ip). The EDL were collected and stored at −80°C for RNA extraction and gene expression assays.

Cell culture. C_2C_{12} mouse myoblasts (American Type Culture Collection, Manassas, VA) were plated at either 8,000 or 10,000 cells/cm^2, depending upon the laboratory, and cultured in Dulbecco's modified Eagle's medium (DMEM; Sigma-Aldrich, St. Louis, MO) with 10% fetal bovine serum (FBS) and 1% penicillin-streptomycin. For differentiation, upon ~80% confluency, differentiation medium (DMEM, 2% horse serum, 1% penicillin-streptomycin) was added, and cells were cultured for 4–6 days into multinucleated myotubes with media changes occurring every other day. Cell line authentication and mycoplasma contamination analysis were not performed apart from initial testing by the vendor company.

RNA isolation and real-time PCR. Total RNA was extracted from C_2C_{12} cells for *Fgf* gene expression using a Total RNA Mini Kit (IBI Scientific, Peosta, IA) and from isolated intact EDL and soleus muscles from CD-1 mice using a RNeasy Fibrous Tissue Mini Kit (Qiagen,Valencia, CA). RNA was also extracted from normal littermate (NL) rat and Cy/+ rat EDL ($n = 6$) and C_2C_{12} cells treated with vehicle ($n = 3$–6), 100 ng/ml recombinant mouse FGF23 (R & D Systems, Minneapolis, MN; $n = 6$), or 100 ng/ml recombinant mouse FGF2 (R & D Systems) as a positive control ($n = 3$) using the miRNeasy Mini Kit (Qiagen), as previously reported (6). Premade TaqMan primer/probe sets specific for mouse are as follows: *β-actin* (Mm01205647_g1), *Fgfr1* (Mm00438930_m1), *Fgfr2* (Mm01269930_m1), *Fgfr3* (Mm00433294_m1), *Fgfr4* (Mm01341852_m1), *Fgf23* (Mm00445621_m1), *α-Klotho* (Mm00502002_m1), *Pax7* (Mm01354484_m1), *Myod* (Mm01203489_g1), *Myogenin* (Mm00446195_g1), *Myostatin* (Mm01254559_m1); and for rat: *β-actin* (Rn00667869), *Fgfr1* (Rn00577234), *Fgfr4* (Rn01441815), and *α-Klotho* (Rn00580123_m1) were utilized (Applied Biosystems, Foster City, CA). Real-time RT-PCR was performed with the ABI One Step RT-PCR kit using a Rotor-Gene 6000 (Qiagen) or ViiA 7 Real-Time PCR systems (Applied Biosystems). The cycle threshold (C_T) value was determined for each gene, and gene expression levels were calculated by comparing $2^{-\Delta C_T}$ or $2^{-\Delta\Delta C_T}$ values, using β-actin as the housekeeping gene, as previously reported (6, 11, 52).

C_2C_{12} cell proliferation. Proliferation was measured with multiple techniques using undifferentiated and differentiated C_2C_{12} cells. Cells were treated with vehicle, FGF23 at various concentrations (2–100 ng/ml), FGF23 + 1 μg/ml soluble-Klotho (R & D Systems), or FGF2 (50–100 ng/ml) as a positive control for 24, 48, or 72 h. Proliferation was measured in 96-well plates using the CellTiter 96 AQueous One kit (Promega, Madison, WI) according to the manufacturer's instructions ($n = 3$; 3 separate experiments), MTT assay ($n = 4$; repeated twice), or 24-well plates using hemocytometer-based cell counting ($n = 3$; repeated twice). MTT assay was performed as previously described (31). Briefly, MTT reagent (Sigma-Aldrich) was added as 10% of the total volume in each well, with 1 h of incubation in a cell culture incubator. The media was aspirated and isopropanol added (100 μl/well), and the plate was then placed on a shaker with vigorous shaking for 0.5 h. Optical density was read at 570 nm with reference at 650 nm. For cell counting, cells were rinsed twice with 1 ml of PBS per well and 0.25 ml trypsin was added per well to detach cells (8 min incubation in cell culture incubator). 0.25 ml growth media was then added to inactivate trypsin and cells were evenly suspended by gentle pipetting before counting on the hemocytometer.

Oxidative stress. C_2C_{12} cells were induced to differentiate and treated with FGF23 (100 ng/ml) for 24 h. Media levels of an oxidative stress marker, 8-hydroxy-2′-deoxyguanosine (8-OHdG), were measured using a DNA damage ELISA kit (Enzo Life Sciences, Farmingdale, NY) ($n = 6$).

Alteration of $[Ca^{2+}]_i$ in C_2C_{12} cells. C_2C_{12} myotubes differentiated for 6 days were loaded with 10 μM fluo-4-AM (Invitrogen, Carlsbad, CA) and imaged, as previously described (52). Briefly, dishes were imaged on an Olympus IX51 (Olympus, Melville, NY) inverted microscope using the ×40 objective, and $[Ca^{2+}]_i$ transients were monitored at room temperature in response to treatments. Fluo-4 was excited using an EXFO X-cite metal halide light source (Mississauga, ON, Canada) and FITC Semrock Bright Line (Rochester, NY) filter set, and the emission signal was captured with a high-resolution charge-coupled device camera (Hammamatsu Photonics, Bridgewater, NJ). Fluorescence data were recorded into Slidebook version 6.0 ratiometric software (Intelligent Imaging Innovations, Denver, CO), and background fluorescence was subtracted.

For determination of acute effects of FGF23 on $[Ca^{2+}]_i$, myotubes were perfused with vehicle (Ringer's buffer) or FGF23 (20 ng/ml) for 10 min, followed by KCl (80 mM) and caffeine (20 mM) as positive controls. Myotubes also received prolonged treatment with FGF23 (20 ng/ml) 24 h before imaging or for the entire 6 days of differentiation to determine whether FGF23 alters depolarization-induced Ca^{2+} release and Ca^{2+}-induced Ca^{2+} release functions, as assessed by perfusion with KCl (80 mM) and caffeine (20 mM), respectively. Individual myotube fluorescence measurements were averaged for each dish ($n = 3$–6 dishes/group, with 5–11 myotubes/dish averaged).

Using a different technique to assess $[Ca^{2+}]_i$, C_2C_{12} myotubes were labeled with Rhod-3 using a Rhod-3 Calcium Imaging kit (Molecular Probe, Carlsbad, CA) for 30 min. FGF23 (100 ng/ml) was then added to the cells for 4 h and the change in $[Ca^{2+}]_i$ in C_2C_{12} cells assessed by fluorescence using the CLARIOstar high-performance microplate reader (BMG Labtech, Cary, NC) ($n = 6$).

Ex vivo skeletal muscle contractility. EDL and soleus muscles were removed from 3- to 5-mo-old CD-1 mice for contractility analysis, as previously described (34). Stimulatory voltage was provided by a S88X dual-pulse digital stimulator (100 V, pulse duration, 1 ms; train duration, 500 ms; Grass Products, West Warwick, RI). EDL and soleus maximal and half-maximal contractions were elicited at high- and low-frequency stimulation, respectively (200 and 100 Hz for EDL; 140–160 and 40 Hz for soleus) (13a) in a modified Krebs-Henseleit buffer (containing in mM: 118 NaCl, 5 KCl, 1 $MgCl_2$, 1 NaH_2PO_4, 25 $NaHCO_3$, 2.5 $CaCl_2$, 10 glucose, pH 7.44) at 37°C for 20 min (2-min rest interval). FGF23 at 9 ng/ml ($n = 6$), 100 ng/ml ($n = 3$–5), or vehicle ($n = 10$) was then directly added to the muscle contractility chambers, and force was monitored for an additional 30 min to determine the effect of FGF23 on force generation properties. The muscles were next stimulated to contract with frequencies ranging from 1 to 220 Hz to generate the force-frequency relationship. To induce fatigue, the muscles were next stimulated at maximal and half-maximal force for 5 min with a rest interval of 2 s. Immediately following the fatiguing protocol, the muscles were allowed a 30-min recovery period while contracting at maximal and half-maximal force, followed by 5 mM caffeine addition to the muscle contractility chambers to probe Ca^{2+} availability during excitation-contraction coupling (3, 56). In an additional set of positive control experiments, maximal and half-maximal contractile force was measured in EDL and soleus muscles during 15 min of incubation with the ryanodine receptor potentiator caffeine (10 mM) or the ryanodine receptor antagonist ryanodine (5 μM). A PowerLab/LabChart Software system (ADInstruments, Colorado Springs, CO) was used to store and analyze force data.

Isolated heart contractility. Isolated heart contractility was performed as previously described (19, 51, 52, 55). Briefly, hearts from 3-mo-old male CD-1 mice were carefully removed and placed into Ringer's solution (pH 7.4). Atria were then removed, and the intact ventricular muscle was attached to small

metallic clips hung vertically from a force transducer (ADInstruments) between bipolar platinum-stimulating electrodes and suspended in 25-ml glass tissue chambers (ADInstruments). Heart muscles were superfused with Ringer's solution continuously bubbled with 100% O_2 at room temperature. Hearts were stretched to the length of maximum force development and paced at 1 Hz (5-ms pulse duration, 20–30 V; Grass Technologies stimulator SD9; Grass Technologies, Quincy, MA). After a stable baseline was obtained, hearts were treated with either vehicle ($n = 4$) or FGF23 (9 ng/ml; $n = 6$) for 30 min while contractile force output was monitored. FGF23 from both laboratories was tested with similar results; therefore, the data were grouped together. The contractile data were recorded and analyzed on the LabChart 6 software (ADInstruments). Waveform changes were analyzed for peak contraction force (mN) and presented as fold change from baseline force.

Statistics. GraphPad Prism 5.02 (GraphPad, La Jolla, CA) and SPSS statistics 24 (IBM, Armonk, NY) were used to conduct all statistical analyses. In vitro cell studies were analyzed with either a two-tailed *t*-test for single comparisons or one-way ANOVA, followed by Bonferroni post hoc analysis for multiple comparisons. Ex vivo skeletal muscle contractility data were analyzed using a two-way ANOVA, followed by Bonferroni post hoc analysis. Isolated heart contractility data were analyzed using a two-tailed *t*-test. $P < 0.05$ was considered the threshold for significance. Data are shown as means ± SE.

RESULTS

Fgf receptor expression in skeletal muscle tissue and C_2C_{12} myocytes. We found expression of *Fgfr1*, *r2*, *r3*, *r4*, and *α-Klotho* in EDL and soleus muscles from CD-1 mice using real-time RT-PCR (Fig. 1). We also tested the expression of *Fgf23* and found it to be at relatively low levels in CD-1 muscle tissues (Fig. 1). The order of gene expression in the EDL muscles of CD-1 mice was *R1>R3/R4>α-Klotho>R2/FGF23*, whereas in soleus muscles the expression order was *R1>R3/R4>R2> α-Klotho/FGF23*. Furthermore, we demonstrated *Fgfr1–4* and *α-Klotho* expression in C_2C_{12} myoblasts and myotubes (Fig. 1). In C_2C_{12} cells, the order of expression was *R1>R4>R3>R2>α-Klotho/FGF23*. In the Cy/+ animal model of CKD, there was an increase in *Fgfr4* compared with normal littermates (NL) but no significant difference in the expression of *Fgfr1* and *α-Klotho* (Fig. 2).

Cellular growth/proliferation. In the heart, FGF23 has direct FGFR4-mediated effects upon cardiomyocyte hypertrophy and contractility (18, 19), and FGFR1 and R4 have been shown to regulate skeletal muscle myogenesis (47, 49, 59). Therefore, we tested the effects of FGF23 upon cellular growth pathways related to proliferation and regeneration in vitro. There was no significant cell proliferation difference in C_2C_{12} myoblasts and myotubes treated with FGF23 (100 ng/ml) and FGF23 (100 ng/ml) + soluble-Klotho (1 μg/ml) for 24 and 48 h (Fig. 3, *A* and *B*). The lack of cell proliferation was confirmed by MTT assay and hemocytometer-based cell counting (Fig. 3, *C* and *D*) of C_2C_{12} myoblasts treated with FGF23 (2–50 ng/ml) for 24, 48, and 72 h. The positive control FGF2 induced proliferation similar to what has previously been observed (4).

Myogenic gene expression. FGF23 (100 ng/ml) treatment for 24 or 48 h had no effect on the expression of *Pax7* (muscle stem cell quiescence), *Myod* (cell activation), and *Myogenin* (cell differentiation) in C_2C_{12} myotubes (Fig. 4, *A–C*). Treatment of FGF23 (100 ng/ml) also had no effect on *Myostatin* expression, which is a negative regulator of skeletal muscle hypertrophy (Fig. 4*D*). In positive control experiments utilizing FGF2, gene expression of *Pax7* increased, whereas *Myod, Myogenin*, and *Myostatin* expression was reduced after 48-h treatment in differentiated C_2C_{12} myotubes (Fig. 4*E*). FGF2-treated cells have a "critical boundary" of 16 to 20 h after plating that enhances cell progression through one round of cell division (50). After the critical boundary, FGF2 represses myogenic gene expression, which is consistent with our 48-h results (10, 20).

In vitro oxidative stress in C_2C_{12} myotubes. Previously, we have found elevated markers of oxidative

stress in muscles of the Cy/+ rat model for CKD (6). Moreover, we have shown previously that FGF23 impairs cardiovascular function, specifically endothelium-dependent vasorelaxation, by increasing superoxide levels (45). Because superoxide metabolism is a generator of reactive oxygen species, we assessed the presence of oxidative stress via 8-OHdG levels (marker of DNA oxidation). There was no evidence of increased oxidative stress following 24-h treatment of FGF23 (100 ng/ml), as demonstrated by no difference in 8-OHdG levels in culture media from C_2C_{12} myotubes (Fig. 4*F*).

Alteration of $[Ca^{2+}]_i$ in C_2C_{12} myotubes. We have previously found that FGF23 can directly increase $[Ca^{2+}]_i$ in primary cardiac myocytes (52). However, acute exposure of FGF23 (20 ng/ml) did not elicit a significant change in myotube $[Ca^{2+}]_i$ as measured by fluo-4 based epifluorescence microscopy of individual myotubes (Fig. 5*A–C*). As expected, acute treatments with 80 mM KCl (depolarization-induced Ca^{2+} release) and 20 mM caffeine (Ca^{2+}-induced Ca^{2+} release) yielded 6.1 ± 0.5 to 7.4 ± 0.6 fold increases in $[Ca^{2+}]_i$, respectively. Moreover, 24 h and long-term 6 days treatment with FGF23 in developing C_2C_{12} myotubes did not significantly alter responses to perfusion with KCl (80 mM) and caffeine (20 mM) compared with vehicle treated cells (Fig. 5*D*). Using Rhod-3 plate readings, following 4 h of FGF23 treatment (100ng/ml), there was no significant difference in C_2C_{12} myotube $[Ca^{2+}]_i$ compared with vehicle (Fig. 5*E*).

Ex vivo skeletal muscle contractility. Contractile parameters of isolated EDL and soleus muscles were assessed at physiological temperature (37°C) after acute treatments of FGF23 (9–100 ng/ml). FGF23 had no effect upon maximal contractile force or force-frequency relationship in the EDL (Fig. 6, *A–C*) and soleus (Fig. 7, *A* and *B*). Furthermore, there was no difference following acute FGF23 treatment (9–100 ng/ml) in the rate of fatigue, recovery from fatigue, or recovery from fatigue in the presence of 5 mM caffeine at maximal contractile force in the EDL (Fig. 6, *D* and *E*) and soleus (Fig. 7, *C* and *D*). We also tested force generation properties, rate of fatigue, recovery from fatigue, and recovery from fatigue in the presence of 5 mM caffeine at half-maximal contractile force in EDL (Fig. 6, *F–H*) and soleus (Fig. 7, *E–G*) and found no effect with FGF23. Furthermore, the rate of force development and relaxation at maximal and half-maximal force was unaffected following FGF23 treatments (data not shown). In positive control experiments, EDL and soleus muscle preparations were responsive to caffeine (10 mM) and ryanodine (5 μM) treatment, resulting in significant force potentiation or diminishment, respectively (Figs. 6*I* and 7*H*).

Isolated heart contractility. We confirmed the bioactivity of the FGF23 utilized in this study by exposing isolated whole heart from mice to FGF23 and monitoring contractility ex vivo. Exposure to FGF23 resulted in a statistically significant 1.7-fold increase in contractile force output within 30 min compared with vehicle treatment (Fig. 8, *A* and *B*). These results are in agreement with our previously published findings of FGF23-dependent enhancement of contractility in left ventricular muscle strips (19, 52).

DISCUSSION

Elevated serum FGF23 has been associated with skeletal muscle weakness in conditions such as CKD (15, 16, 23, 48) and genetic hypophosphatemic rickets (5, 18, 55). Given the direct effects of FGF23 on the heart and cardiac myocytes shown by our group and others (14, 24, 52), we tested the hypothesis that FGF23 would have a direct effect on skeletal muscle. Despite finding that *Fgfr1* to *-4* and *α-Klotho* were expressed in skeletal muscle and C_2C_{12} cells, FGF23 treatments failed to modulate C_2C_{12} myoblast proliferation, regulation of myogenesis, oxidative stress, $[Ca^{2+}]_I$, or ex vivo isometric force in whole skeletal muscles. FGF23 concentrations utilized in these studies follow similar concentration levels used by our group and other previous studies and fall within the range measured in the serum during CKD/hemodialysis and hypophosphatemic rickets (12, 14, 22, 44, 45, 52). These experiments were performed by two independent laboratories, which further lends support to the lack of a direct effect of FGF23 on skeletal muscle under the conditions tested.

In other tissues, FGF23 signaling occurs through one or more of the FGFRs (R1, R2, R3, or R4) with or without participation of the coreceptor α-Klotho (18, 28, 39, 42). To verify the potential for direct FGF23-skeletal muscle communication, we found the expression of all four *Fgfrs* and *α-Klotho* in the EDL, soleus, and C_2C_{12} cells consistent with previous findings (25, 35, 47, 49). In skeletal muscle, activation of R1 and R4 has previously been shown to induce satellite cell proliferation and regeneration (47, 49, 57, 59). Another member of the FGF family, basic FGF (FGF2), signals (in a klotho-independent manner) via binding of FGFR1 and heparan sulfate in skeletal muscle cells (38) and increases cell proliferation (57). Because we demonstrated a similar increase in cellular proliferation in response to FGF2 in our studies, this indicates that FGFR1 activation was functional in our cell model and that a FGFR response may occur, but not from FGF23 treatments.

The process of skeletal muscle regeneration occurs through coordinated expression of myogenic regulatory transcription factors (i.e., *Pax7*, *Myod*, and *Myogenin*) (41). In models of surgically induced CKD, it has been reported that muscle satellite cell activity is impaired concurrent with downregulation of *Myod*, *Myf5*, and *Myogenin* expression (58). While in the terminal stages of a more slowly progressing model of CKD-mineral bone disorder (Cy/+ rat), skeletal muscle regeneration has been shown to be activated, which may reduce the quiescent satellite cell pool (6). However, we found that FGF23 treatments did not alter transcription factor expression in C_2C_{12} differentiated myotubes. This lack of effect on regulatory genes would further support the absence of change in regeneration as a direct response to FGF23.

We next investigated the potential interaction with oxidative stress. Increased oxidative stress is associated with CKD progression and may play a major role in development of cardiovascular pathogenesis during CKD (13). Specifically, FGF23 levels are correlated with oxidative stress in stage 5 CKD patients on hemodialysis (32). We have previously shown that FGF23 directly increases oxidative stress markers and promotes endothelial dysfunction in mouse aortic rings (45). Oxidative stress is also believed to underlie conditions of muscle wasting in multiple disease states through a number of pathways, including inhibition of Akt/mTORC1 signaling, increased atrogin-1/MuRF-1 expression, and upregulation of *Myostatin* (36, 37). Skeletal muscles of Cy/+ rats with end-stage renal failure display significantly elevated oxidative stress markers and oxidative damage to myofibrils (6). However, in the present study, we did not observe an increase in oxidative stress from muscle cells treated with high amounts of FGF23 for 24 h, nor did we observe a significant change in *Myostatin* expression, which may be altered by increased oxidative stress.

Changes in skeletal muscle strength may also be due to changes in muscle function; therefore, we investigated whether FGF23 could alter Ca^{2+} handling and contractility. Our group has shown in the Cy/+ rat model of CKD several skeletal muscle functional abnormalities in parallel with elevated serum FGF23, including decreased hind limb maximal torque production and prolonged muscle relaxation (33). In rats with nephrectomy-induced CKD, skeletal muscles had delayed time to reach peak contraction force and time to relaxation, increased fatigability, and altered force-frequency relationships (48). The mechanism underlying these impairments is unknown but may result from dysfunction of Ca^{2+} handling. Our group has shown that FGF23 directly increases cardiac contractility and $[Ca^{2+}]_i$ in isolated primary cardiomyocytes (52), and Kao et al. (24) have shown that FGF23 alters sarcoplasmic reticulum (SR) Ca^{2+} content and handling in HL-1 atrial cells and thus may ultimately contribute to Ca^{2+} overload and cardiac dysfunction in CKD (29). Interestingly, FGF23 did not alter $[Ca^{2+}]_i$ of isolated myotubes or the contractile force, rate of contractile force development or relaxation, force-frequency relationship or rate of fatigue/recovery of isolated EDL, or soleus skeletal muscles after acute treatment with FGF23. Thus, in these studies, our ex vivo contractility experiments in CD1 mice failed to recapitulate the skeletal muscle dysfunction observed in CKD.

The lack of an FGF23 effect was not due to cell/tissue unresponsiveness since positive control experiments showed a response in our in vitro and ex vivo models. Similarly, it was also not due to inactive FGF23, as

exposure of isolated heart muscle to the same FGF23 resulted in a 1.7 fold increase in contractile force, similar to what we have found previously (19, 52). However, the absence of a response may be due to differences between cardiac and skeletal muscle FGF receptor activation/signaling or Ca^{2+} handling, lack of other substances that work in concert with FGF23, or FGF23 treatment conditions. In regard to Ca^{2+} handling, previous studies have elucidated a role of the cardiac L-type channel Ca^{2+} currents in the FGF23-induced increase in $[Ca^{2+}]_i$ in cardiac myocytes (24, 52). There are key distinctions between skeletal muscle and cardiac-specific L-type channel isoforms (skeletal muscle contains $Ca_V1.1$ and cardiac muscle contains $Ca_V1.2$), L-type channel Ca^{2+} conductance capabilities and functionality in excitation-contraction coupling (ECC), and ryanodine receptors (skeletal muscle contains RYR1 and cardiac muscle contains RYR2), which may account for different responses (7, 27).

In pathologies with FGF23 elevation, it is also possible that additional endogenous substances may be required to act in concert with FGF23 or isolated from FGF23 to induce skeletal muscle weakness. In CKD, the origins of muscle weakness are further confounded by various factors, including an increase in circulating toxic uremic factors, inflammatory cytokines, metabolic acidosis, anemia, and insulin resistance, among others (2). Moreover, in CKD, secondary hyperparathyroidism is associated with skeletal muscle decline, possibly through direct effects of parathyroid hormone (46) and/or reduction of skeletal muscle $1,25(OH)_2D$ uptake and retention (1). In models of ADHR and XLH, skeletal muscle weakness is related to the condition of rickets, which does not occur solely with isolated FGF23 elevation but rather with hypophosphatemia and impaired $1,25(OH)_2D$ metabolism due to the increased FGF23. These factors may in part play a role in the muscle weakness we observed in testing the Dmp1-null mouse model of elevated FGF23 (55). Specifically, low levels of $1,25(OH)_2D$ have been suggested to impair the musculoskeletal system with associations of reduced skeletal muscle mass, strength, and physical function (17).

There are some limitations of these experimental models. Although we utilized a FGF23 concentration and incubation protocol similar to that of previous studies in cardiac muscle (14, 52), it is possible that FGF23 exerts effects on skeletal muscle function with more prolonged exposure to elevated FGF23 or with muscle under greater physiological stress such as multiple or longer bouts of fatigue/recovery. It is also possible in our acute skeletal muscle studies that FGF23 was not able to diffuse into the muscle tissue as it would in the normal circulation. Additionally, the absence of a response with treatment in isolated cells would support a lack of effect in skeletal muscle. Although the goal of this study was to determine direct effects of FGF23 in vitro and ex vivo without other confounding factors, further in vivo experiments are warranted to expose muscles to FGF23 over longer periods. Given the multitude of targets for this endocrine and paracrine factor, alterations in phosphate, vitamin D, Ca^{2+}, and parathyroid hormone, among others, would need to be carefully controlled to differentiate between direct and indirect effects of FGF23.

In conclusion, our in vitro and ex vivo results suggest that in contrast to cardiac muscle, increased levels of FGF23 alone may not directly alter skeletal muscle myoblast proliferation, myotube development, Ca^{2+} handling, or acute skeletal muscle contractility.

GRANTS

This study was supported by National Institute on Aging Grant P01-AG-039355 to M. J. Wacker, M. Brotto, and S. L. Dallas, National Institute of Diabetes and Digestive and Kidney Diseases Grant 1-K08-DK-110429 to K. G. Avin, and National Institute of Arthritis and Musculoskeletal and Skin Diseases Grant R01-AR-070175 and Veterans Affairs Merit Award BX001471 to S. M. Moe.

DISCLOSURES

No conflicts of interest, financial or otherwise, are declared by the authors.

AUTHOR CONTRIBUTIONS

K.G.A., J.A.V., N.X.C., K.W., C.D.T., M.B., S.L.D., S.M.M., and M.J.W. conceived and designed research; K.G.A., J.A.V., N.X.C., and K.W. performed experiments; K.G.A., J.A.V., N.X.C., M.J.W., and K.W. analyzed data; K.G.A., J.A.V., N.X.C., K.W., C.D.T., M.B., S.L.D., S.M.M., and M.J.W. interpreted results of experiments; K.G.A., J.A.V., N.X.C., and K.W. prepared figures; K.G.A., M.J.W., and J.A.V. drafted manuscript; K.G.A., J.A.V., N.X.C., K.W., C.D.T., M.B., S.L.D., S.M.M., and M.J.W. edited and revised manuscript; K.G.A., J.A.V., N.X.C., K.W., C.D.T., M.B., S.L.D., S.M.M., and M.J.W. approved final version of manuscript.

References

1. Abboud M, Rybchyn MS, Liu J, Ning Y, Gordon-Thomson C, Brennan-Speranza TC, Cole L, Greenfield H, Fraser DR, Mason RS. The effect of parathyroid hormone on the uptake and retention of 25-hydroxyvitamin D in skeletal muscle cells. J Steroid Biochem Mol Biol 173: 173–179, 2017. doi:10.1016/j.jsbmb.2017.01.001. [PubMed: 28104493] [CrossRef: 10.1016/j.jsbmb.2017.01.001]

2. Adams GR, Vaziri ND. Skeletal muscle dysfunction in chronic renal failure: effects of exercise. Am J Physiol Renal Physiol 290: F753–F761, 2006. doi:10.1152/ajprenal.00296.2005. [PubMed: 16527920] [CrossRef: 10.1152/ajprenal.00296.2005]

3. Allen DG, Westerblad H. The effects of caffeine on intracellular calcium, force and the rate of relaxation of mouse skeletal muscle. J Physiol 487: 331–342, 1995. doi:10.1113/jphysiol.1995.sp020883. [PMCID: PMC1156576] [PubMed: 8558467] [CrossRef: 10.1113/jphysiol.1995.sp020883]

4. Allen RE, Boxhorn LK. Regulation of skeletal muscle satellite cell proliferation and differentiation by transforming growth factor-beta, insulin-like growth factor I, and fibroblast growth factor. J Cell Physiol 138: 311–315, 1989. doi:10.1002/jcp.1041380213. [PubMed: 2918032] [CrossRef: 10.1002/jcp.1041380213]

5. Aono Y, Hasegawa H, Yamazaki Y, Shimada T, Fujita T, Yamashita T, Fukumoto S. Anti-FGF-23 neutralizing antibodies ameliorate muscle weakness and decreased spontaneous movement of Hyp mice. J Bone Miner Res 26: 803–810, 2011. doi:10.1002/jbmr.275. [PubMed: 20939065] [CrossRef: 10.1002/jbmr.275]

6. Avin KG, Chen NX, Organ JM, Zarse C, O'Neill K, Conway RG, Konrad RJ, Bacallao RL, Allen MR, Moe SM. Skeletal muscle regeneration and oxidative stress are altered in chronic kidney disease. PLoS One 11: e0159411, 2016. doi:10.1371/journal.pone.0159411. [PMCID: PMC4972446] [PubMed: 27486747] [CrossRef: 10.1371/journal.pone.0159411]

7. Bannister RA. Bridging the myoplasmic gap II: more recent advances in skeletal muscle excitation-contraction coupling. J Exp Biol 219: 175–182, 2016. doi:10.1242/jeb.124123. [PubMed: 26792328] [CrossRef: 10.1242/jeb.124123]

8. Bonewald LF, Wacker MJ. FGF23 production by osteocytes. Pediatr Nephrol 28: 563–568, 2013. doi:10.1007/s00467-012-2309-3. [PMCID: PMC3582753] [PubMed: 22983423] [CrossRef: 10.1007/s00467-012-2309-3]

10. Brunetti A, Goldfine ID. Differential effects of fibroblast growth factor on insulin receptor and muscle specific protein gene expression in BC3H-1 myocytes. Mol Endocrinol 4: 880–885, 1990. doi:10.1210/mend-4-6-880. [PubMed: 2172794] [CrossRef: 10.1210/mend-4-6-880]

11. Chen NX, O'Neill KD, Allen MR, Newman CL, Moe SM. Low bone turnover in chronic kidney disease is associated with decreased VEGF-A expression and osteoblast differentiation. Am J Nephrol 41:

464–473, 2015. doi:10.1159/000438461. [PubMed: 26228644] [CrossRef: 10.1159/000438461]

12. Clinkenbeard EL, Cass TA, Ni P, Hum JM, Bellido T, Allen MR, White KE. Conditional deletion of murine Fgf23: interruption of the normal skeletal responses to phosphate challenge and rescue of genetic hypophosphatemia. J Bone Miner Res 31: 1247–1257, 2016. doi:10.1002/jbmr.2792. [PMCID: PMC4891276] [PubMed: 26792657] [CrossRef: 10.1002/jbmr.2792]

13. Cottone S, Lorito MC, Riccobene R, Nardi E, Mulè G, Buscemi S, Geraci C, Guarneri M, Arsena R, Cerasola G. Oxidative stress, inflammation and cardiovascular disease in chronic renal failure. J Nephrol 21: 175–179, 2008. [PubMed: 18446711]

13a. de Paula Brotto MA, Nosek TM, Kolbeck RC. Influence of ageing on the fatigability of isolated mouse skeletal muscles from mature and aged mice. Exp Physiol 87: 77–82, 2002. doi:10.1113/eph8702224. [PubMed: 11805861] [CrossRef: 10.1113/eph8702224]

14. Faul C, Amaral AP, Oskouei B, Hu MC, Sloan A, Isakova T, Gutiérrez OM, Aguillon-Prada R, Lincoln J, Hare JM, Mundel P, Morales A, Scialla J, Fischer M, Soliman EZ, Chen J, Go AS, Rosas SE, Nessel L, Townsend RR, Feldman HI, St. John Sutton M, Ojo A, Gadegbeku C, Di Marco GS, Reuter S, Kentrup D, Tiemann K, Brand M, Hill JA, Moe OW, Kuro-O M, Kusek JW, Keane MG, Wolf M. FGF23 induces left ventricular hypertrophy. J Clin Invest 121: 4393–4408, 2011. doi:10.1172/JCI46122. [PMCID: PMC3204831] [PubMed: 21985788] [CrossRef: 10.1172/JCI46122]

15. Foley RN, Wang C, Ishani A, Collins AJ, Murray AM. Kidney function and sarcopenia in the United States general population: NHANES III. Am J Nephrol 27: 279–286, 2007. doi:10.1159/000101827. [PubMed: 17440263] [CrossRef: 10.1159/000101827]

16. Fried LF, Lee JS, Shlipak M, Chertow GM, Green C, Ding J, Harris T, Newman AB. Chronic kidney disease and functional limitation in older people: health, aging and body composition study. J Am Geriatr Soc 54: 750–756, 2006. doi:10.1111/j.1532-5415.2006.00727.x. [PubMed: 16696739] [CrossRef: 10.1111/j.1532-5415.2006.00727.x]

17. Girgis CM, Clifton-Bligh RJ, Hamrick MW, Holick MF, Gunton JE. The roles of vitamin D in skeletal muscle: form, function, and metabolism. Endocr Rev 34: 33–83, 2013. doi:10.1210/er.2012-1012. [PubMed: 23169676] [CrossRef: 10.1210/er.2012-1012]

18. Grabner A, Amaral AP, Schramm K, Singh S, Sloan A, Yanucil C, Li J, Shehadeh LA, Hare JM, David V, Martin A, Fornoni A, Di Marco GS, Kentrup D, Reuter S, Mayer AB, Pavenstädt H, Stypmann J, Kuhn C, Hille S, Frey N, Leifheit-Nestler M, Richter B, Haffner D, Abraham R, Bange J, Sperl B, Ullrich A, Brand M, Wolf M, Faul C. Activation of cardiac fibroblast growth factor receptor 4 causes left ventricular hypertrophy. Cell Metab 22: 1020–1032, 2015. doi:10.1016/j.cmet.2015.09.002. [PMCID: PMC4670583] [PubMed: 26437603] [CrossRef: 10.1016/j.cmet.2015.09.002]

19. Grabner A, Schramm K, Silswal N, Hendrix M, Yanucil C, Czaya B, Singh S, Wolf M, Hermann S, Stypmann J, Di Marco GS, Brand M, Wacker MJ, Faul C. FGF23/FGFR4-mediated left ventricular hypertrophy is reversible. Sci Rep 7: 1993, 2017. doi:10.1038/s41598-017-02068-6. [PMCID: PMC5434018] [PubMed: 28512310] [CrossRef: 10.1038/s41598-017-02068-6]

20. Gutiérrez J, Brandan E. A novel mechanism of sequestering fibroblast growth factor 2 by glypican in lipid rafts, allowing skeletal muscle differentiation. Mol Cell Biol 30: 1634–1649, 2010. doi:10.1128/MCB.01164-09. [PMCID: PMC2838066] [PubMed: 20100867] [CrossRef: 10.1128/MCB.01164-09]

21. Imanishi Y, Inaba M, Nakatsuka K, Nagasue K, Okuno S, Yoshihara A, Miura M, Miyauchi A, Kobayashi K, Miki T, Shoji T, Ishimura E, Nishizawa Y. FGF-23 in patients with end-stage renal disease on

hemodialysis. Kidney Int 65: 1943–1946, 2004. doi:10.1111/j.1523-1755.2004.00604.x. [PubMed: 15086938] [CrossRef: 10.1111/j.1523-1755.2004.00604.x]

22. Isakova T. Fibroblast growth factor 23 and adverse clinical outcomes in chronic kidney disease. Curr Opin Nephrol Hypertens 21: 334–340, 2012. doi:10.1097/MNH.0b013e328351a391. [PMCID: PMC3353875] [PubMed: 22487610] [CrossRef: 10.1097/MNH.0b013e328351a391]

23. Johansen KL, Shubert T, Doyle J, Soher B, Sakkas GK, Kent-Braun JA. Muscle atrophy in patients receiving hemodialysis: effects on muscle strength, muscle quality, and physical function. Kidney Int 63: 291–297, 2003. doi:10.1046/j.1523-1755.2003.00704.x. [PubMed: 12472795] [CrossRef: 10.1046/j.1523-1755.2003.00704.x]

24. Kao YH, Chen YC, Lin YK, Shiu RJ, Chao TF, Chen SA, Chen YJ. FGF-23 dysregulates calcium homeostasis and electrophysiological properties in HL-1 atrial cells. Eur J Clin Invest 44: 795–801, 2014. doi:10.1111/eci.12296. [PubMed: 24942561] [CrossRef: 10.1111/eci.12296]

25. Kuro-o M, Matsumura Y, Aizawa H, Kawaguchi H, Suga T, Utsugi T, Ohyama Y, Kurabayashi M, Kaname T, Kume E, Iwasaki H, Iida A, Shiraki-Iida T, Nishikawa S, Nagai R, Nabeshima YI. Mutation of the mouse klotho gene leads to a syndrome resembling ageing. Nature 390: 45–51, 1997. doi:10.1038/36285. [PubMed: 9363890] [CrossRef: 10.1038/36285]

26. Larsson T, Nisbeth U, Ljunggren O, Jüppner H, Jonsson KB. Circulating concentration of FGF-23 increases as renal function declines in patients with chronic kidney disease, but does not change in response to variation in phosphate intake in healthy volunteers. Kidney Int 64: 2272–2279, 2003. doi:10.1046/j.1523-1755.2003.00328.x. [PubMed: 14633152] [CrossRef: 10.1046/j.1523-1755.2003.00328.x]

27. Lee CS, Dagnino-Acosta A, Yarotskyy V, Hanna A, Lyfenko A, Knoblauch M, Georgiou DK, Poché RA, Swank MW, Long C, Ismailov II, Lanner J, Tran T, Dong K, Rodney GG, Dickinson ME, Beeton C, Zhang P, Dirksen RT, Hamilton SL. Ca(2+) permeation and/or binding to CaV1.1 fine-tunes skeletal muscle Ca(2+) signaling to sustain muscle function. Skelet Muscle 5: 4, 2015. doi:10.1186/s13395-014-0027-1. [PMCID: PMC4340672] [PubMed: 25717360] [CrossRef: 10.1186/s13395-014-0027-1]

28. Li H, Martin A, David V, Quarles LD. Compound deletion of Fgfr3 and Fgfr4 partially rescues the Hyp mouse phenotype. Am J Physiol Endocrinol Metab 300: E508–E517, 2011. doi:10.1152/ajpendo.00499.2010. [PMCID: PMC3064005] [PubMed: 21139072] [CrossRef: 10.1152/ajpendo.00499.2010]

29. Moe SM. Calcium as a cardiovascular toxin in CKD-MBD. Bone 100: 94–99, 2017. doi:10.1016/j.bone.2016.08.022. [PMCID: PMC5329167] [PubMed: 27576942] [CrossRef: 10.1016/j.bone.2016.08.022]

30. Moe SM, Chen NX, Seifert MF, Sinders RM, Duan D, Chen X, Liang Y, Radcliff JS, White KE, Gattone VH II. A rat model of chronic kidney disease-mineral bone disorder. Kidney Int 75: 176–184, 2009. doi:10.1038/ki.2008.456. [PMCID: PMC2716076] [PubMed: 18800026] [CrossRef: 10.1038/ki.2008.456]

31. Mosmann T. Rapid colorimetric assay for cellular growth and survival: application to proliferation and cytotoxicity assays. J Immunol Methods 65: 55–63, 1983. doi:10.1016/0022-1759(83)90303-4. [PubMed: 6606682] [CrossRef: 10.1016/0022-1759(83)90303-4]

32. NasrAllah MM, El-Shehaby AR, Osman NA, Fayad T, Nassef A, Salem MM, Sharaf El Din UA. The association between fibroblast growth factor-23 and vascular calcification is mitigated by inflammation

markers. Nephron Extra 3: 106–112, 2013. doi:10.1159/000356118. [PMCID: PMC3843931] [PubMed: 24348506] [CrossRef: 10.1159/000356118]

33. Organ JM, Srisuwananukorn A, Price P, Joll JE, Biro KC, Rupert JE, Chen NX, Avin KG, Moe SM, Allen MR. Reduced skeletal muscle function is associated with decreased fiber cross-sectional area in the Cy/+ rat model of progressive kidney disease. Nephrol Dial Transplant 31: 223–230, 2016. [PMCID: PMC4725390] [PubMed: 26442903]

34. Park KH, Brotto L, Lehoang O, Brotto M, Ma J, Zhao X. Ex vivo assessment of contractility, fatigability and alternans in isolated skeletal muscles. J Vis Exp: e4198, 2012. doi:10.3791/4198. [PMCID: PMC3499085] [PubMed: 23149471] [CrossRef: 10.3791/4198]

35. Phelps M, Stuelsatz P, Yablonka-Reuveni Z. Expression profile and overexpression outcome indicate a role for βKlotho in skeletal muscle fibro/adipogenesis. FEBS J 283: 1653–1668, 2016. doi:10.1111/febs.13682. [PMCID: PMC5070976] [PubMed: 26881702] [CrossRef: 10.1111/febs.13682]

36. Powers SK, Kavazis AN, DeRuisseau KC. Mechanisms of disuse muscle atrophy: role of oxidative stress. Am J Physiol Regul Integr Comp Physiol 288: R337–R344, 2005. doi:10.1152/ajpregu.00469.2004. [PubMed: 15637170] [CrossRef: 10.1152/ajpregu.00469.2004]

37. Powers SK, Morton AB, Ahn B, Smuder AJ. Redox control of skeletal muscle atrophy. Free Radic Biol Med 98: 208–217, 2016. doi:10.1016/j.freeradbiomed.2016.02.021. [PMCID: PMC5006677] [PubMed: 26912035] [CrossRef: 10.1016/j.freeradbiomed.2016.02.021]

38. Rapraeger AC, Krufka A, Olwin BB. Requirement of heparan sulfate for bFGF-mediated fibroblast growth and myoblast differentiation. Science 252: 1705–1708, 1991. doi:10.1126/science.1646484. [PubMed: 1646484] [CrossRef: 10.1126/science.1646484]

39. Rossaint J, Oehmichen J, Van Aken H, Reuter S, Pavenstädt HJ, Meersch M, Unruh M, Zarbock A. FGF23 signaling impairs neutrophil recruitment and host defense during CKD. J Clin Invest 126: 962–974, 2016. doi:10.1172/JCI83470. [PMCID: PMC4767336] [PubMed: 26878171] [CrossRef: 10.1172/JCI83470]

40. Ruppe MD, Zhang X, Imel EA, Weber TJ, Klausner MA, Ito T, Vergeire M, Humphrey JS, Glorieux FH, Portale AA, Insogna K, Peacock M, Carpenter TO. Effect of four monthly doses of a human monoclonal anti-FGF23 antibody (KRN23) on quality of life in X-linked hypophosphatemia. Bonekey Rep 5: 158–162, 2016. doi:10.1016/j.bonr.2016.05.004. [PMCID: PMC4926842] [PubMed: 28326356] [CrossRef: 10.1016/j.bonr.2016.05.004]

41. Shadrin IY, Khodabukus A, Bursac N. Striated muscle function, regeneration, and repair. Cell Mol Life Sci 73: 4175–4202, 2016. doi:10.1007/s00018-016-2285-z. [PMCID: PMC5056123] [PubMed: 27271751] [CrossRef: 10.1007/s00018-016-2285-z]

42. Shalhoub V, Ward SC, Sun B, Stevens J, Renshaw L, Hawkins N, Richards WG. Fibroblast growth factor 23 (FGF23) and alpha-klotho stimulate osteoblastic MC3T3.E1 cell proliferation and inhibit mineralization. Calcif Tissue Int 89: 140–150, 2011. doi:10.1007/s00223-011-9501-5. [PMCID: PMC3135830] [PubMed: 21633782] [CrossRef: 10.1007/s00223-011-9501-5]

43. Sharma S, Joseph J, Chonchol M, Kaufman JS, Cheung AK, Rafeq Z, Smits G, Kendrick J; HOST Investigators . Higher fibroblast growth factor-23 concentrations associate with left ventricular systolic dysfunction in dialysis patients. Clin Nephrol 80: 313–321, 2013. doi:10.5414/CN107991. [PMCID: PMC4018462] [PubMed: 23849306] [CrossRef: 10.5414/CN107991]

44. Shimada T, Urakawa I, Isakova T, Yamazaki Y, Epstein M, Wesseling-Perry K, Wolf M, Salusky IB,

Jüppner H. Circulating fibroblast growth factor 23 in patients with end-stage renal disease treated by peritoneal dialysis is intact and biologically active. J Clin Endocrinol Metab 95: 578–585, 2010. doi:10.1210/jc.2009-1603. [PMCID: PMC2840849] [PubMed: 19965919] [CrossRef: 10.1210/jc.2009-1603]

45. Silswal N, Touchberry CD, Daniel DR, McCarthy DL, Zhang S, Andresen J, Stubbs JR, Wacker MJ. FGF23 directly impairs endothelium-dependent vasorelaxation by increasing superoxide levels and reducing nitric oxide bioavailability. Am J Physiol Endocrinol Metab 307: E426–E436, 2014. doi:10.1152/ajpendo.00264.2014. [PMCID: PMC4154070] [PubMed: 25053401] [CrossRef: 10.1152/ajpendo.00264.2014]

46. Smogorzewski M, Piskorska G, Borum PR, Massry SG. Chronic renal failure, parathyroid hormone and fatty acids oxidation in skeletal muscle. Kidney Int 33: 555–560, 1988. doi:10.1038/ki.1988.33. [PubMed: 3361755] [CrossRef: 10.1038/ki.1988.33]

47. Sogos V, Balaci L, Ennas MG, Dell'era P, Presta M, Gremo F. Developmentally regulated expression and localization of fibroblast growth factor receptors in the human muscle. Dev Dyn 211: 362–373, 1998. doi:10.1002/(SICI)1097-0177(199804)211:4<362::AID-AJA7>3.0.CO;2-F. [PubMed: 9566955] [CrossRef: 10.1002/(SICI)1097-0177(199804)211:4<362::AID-AJA7>3.0.CO;2-F]

48. Tarasuik A, Heimer D, Bark H. Effect of chronic renal failure on skeletal and diaphragmatic muscle contraction. Am Rev Respir Dis 146: 1383–1388, 1992. doi:10.1164/ajrccm/146.6.1383. [PubMed: 1456552] [CrossRef: 10.1164/ajrccm/146.6.1383]

49. Templeton TJ, Hauschka SD. FGF-mediated aspects of skeletal muscle growth and differentiation are controlled by a high affinity receptor, FGFR1. Dev Biol 154: 169–181, 1992. doi:10.1016/0012-1606(92)90057-N. [PubMed: 1426624] [CrossRef: 10.1016/0012-1606(92)90057-N]

50. Tortorella LL, Milasincic DJ, Pilch PF. Critical proliferation-independent window for basic fibroblast growth factor repression of myogenesis via the p42/p44 MAPK signaling pathway. J Biol Chem 276: 13709–13717, 2001. doi:10.1074/jbc.M100091200. [PubMed: 11279003] [CrossRef: 10.1074/jbc.M100091200]

51. Touchberry CD, Bales IK, Stone JK, Rohrberg TJ, Parelkar NK, Nguyen T, Fuentes O, Liu X, Qu CK, Andresen JJ, Valdivia HH, Brotto M, Wacker MJ. Phosphatidylinositol 3,5-bisphosphate (PI(3,5)P2) potentiates cardiac contractility via activation of the ryanodine receptor. J Biol Chem 285: 40312–40321, 2010. doi:10.1074/jbc.M110.179689. [PMCID: PMC3001011] [PubMed: 20947503] [CrossRef: 10.1074/jbc.M110.179689]

52. Touchberry CD, Green TM, Tchikrizov V, Mannix JE, Mao TF, Carney BW, Girgis M, Vincent RJ, Wetmore LA, Dawn B, Bonewald LF, Stubbs JR, Wacker MJ. FGF23 is a novel regulator of intracellular calcium and cardiac contractility in addition to cardiac hypertrophy. Am J Physiol Endocrinol Metab 304: E863–E873, 2013. doi:10.1152/ajpendo.00596.2012. [PMCID: PMC3625783] [PubMed: 23443925] [CrossRef: 10.1152/ajpendo.00596.2012]

53. Veilleux LN, Cheung M, Ben Amor M, Rauch F. Abnormalities in muscle density and muscle function in hypophosphatemic rickets. J Clin Endocrinol Metab 97: E1492–E1498, 2012. doi:10.1210/jc.2012-1336. [PubMed: 22639288] [CrossRef: 10.1210/jc.2012-1336]

54. Veilleux LN, Cheung MS, Glorieux FH, Rauch F. The muscle-bone relationship in X-linked hypophosphatemic rickets. J Clin Endocrinol Metab 98: E990–E995, 2013. doi:10.1210/jc.2012-4146. [PubMed: 23526465] [CrossRef: 10.1210/jc.2012-4146]

55. Wacker MJ, Touchberry CD, Silswal N, Brotto L, Elmore CJ, Bonewald LF, Andresen J, Brotto M.

Skeletal muscle, but not cardiovascular function, is altered in a mouse model of autosomal recessive hypophosphatemic rickets. Front Physiol 7: 173, 2016. doi:10.3389/fphys.2016.00173. [PMCID: PMC4866514] [PubMed: 27242547] [CrossRef: 10.3389/fphys.2016.00173]

56. Wendt IR, Stephenson DG. Effects of caffeine on Ca-activated force production in skinned cardiac and skeletal muscle fibres of the rat. Pflugers Arch 398: 210–216, 1983. doi:10.1007/BF00657153. [PubMed: 6634380] [CrossRef: 10.1007/BF00657153]

57. Yablonka-Reuveni Z, Danoviz ME, Phelps M, Stuelsatz P. Myogenic-specific ablation of Fgfr1 impairs FGF2-mediated proliferation of satellite cells at the myofiber niche but does not abolish the capacity for muscle regeneration. Front Aging Neurosci 7: 85, 2015. doi:10.3389/fnagi.2015.00085. [PMCID: PMC4446549] [PubMed: 26074812] [CrossRef: 10.3389/fnagi.2015.00085]

58. Zhang L, Wang XH, Wang H, Du J, Mitch WE. Satellite cell dysfunction and impaired IGF-1 signaling cause CKD-induced muscle atrophy. J Am Soc Nephrol 21: 419–427, 2010. doi:10.1681/ASN.2009060571. [PMCID: PMC2831855] [PubMed: 20056750] [CrossRef: 10.1681/ASN.2009060571]

59. Zhao P, Caretti G, Mitchell S, McKeehan WL, Boskey AL, Pachman LM, Sartorelli V, Hoffman EP. Fgfr4 is required for effective muscle regeneration in vivo. Delineation of a MyoD-Tead2-Fgfr4 transcriptional pathway. J Biol Chem 281: 429–438, 2006. doi:10.1074/jbc.M507440200. [PMCID: PMC1892582] [PubMed: 16267055] [CrossRef: 10.1074/jbc.M507440200]

Figures and Tables

Fig. 1.

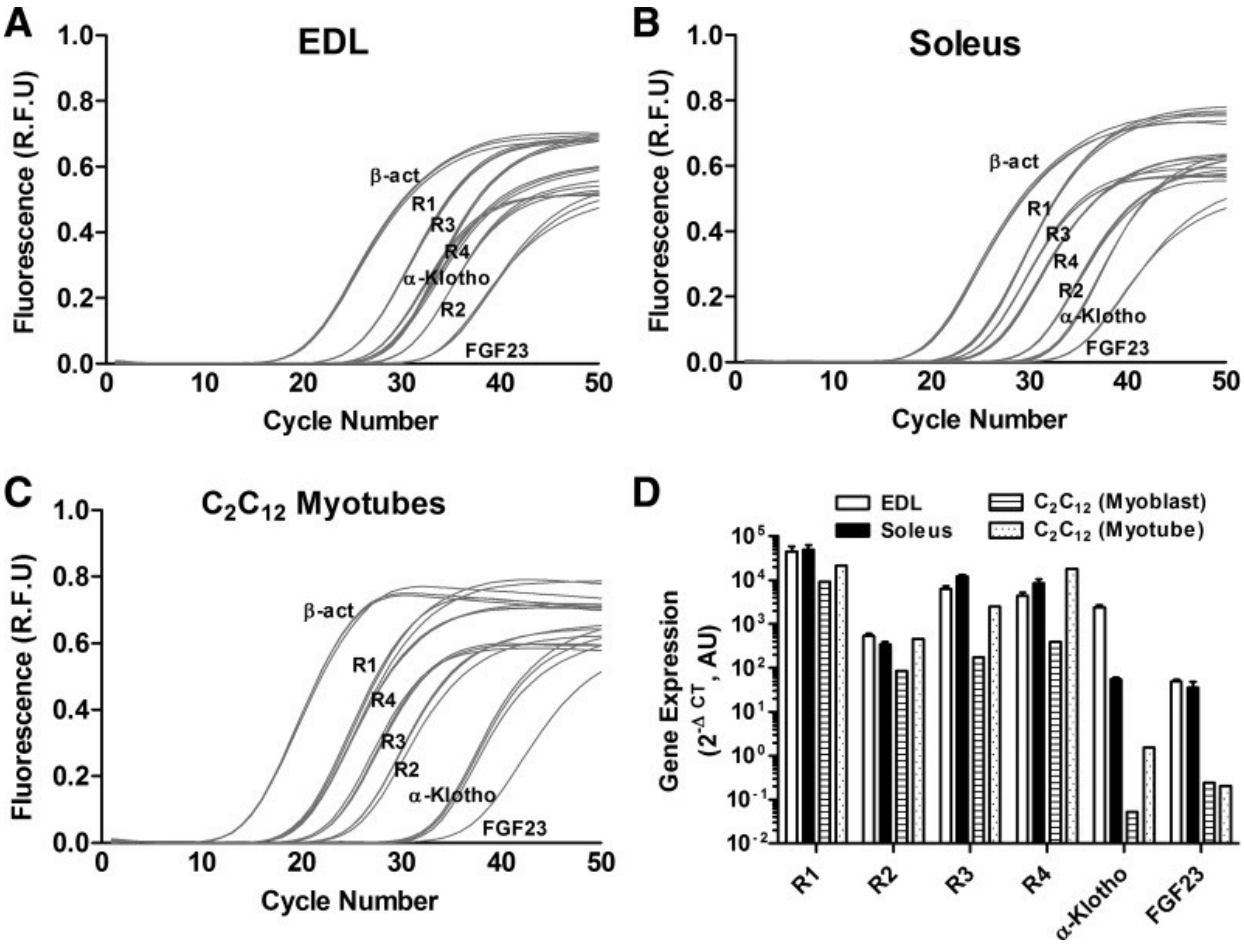

Fibroblasti growth factor (*Fgf*) *receptors* (*Fgfr*), *α-Klotho*, and *Fgf23* are expressed in skeletal muscle. *A–C*: are representative real-time RT-PCR amplification plots showing values of fluorescence at each cycle number of *Fgfr1–4*, *α-Klotho*, and *Fgf23* (each reaction in triplicate) in isolated extensor digitorum longus (EDL; *A*) and soleus (*B*) muscles from 4- to 5-mo-old CD-1 male mice and in differentiated C_2C_{12} myotubes (*C*). *D*: summary data showing average $2^{-\Delta C_T}$ values ($\times 10^6$) of *Fgfr1–4*, *α-Klotho*, and *Fgf23* in EDL and soleus muscles from 4- to 5-mo-old CD-1 male mice ($n = 3$) and in C_2C_{12} myoblasts and myotubes ($n = 1$) expressed relative to *β-actin* on $\log_{10}$ scale.

Fig. 2.

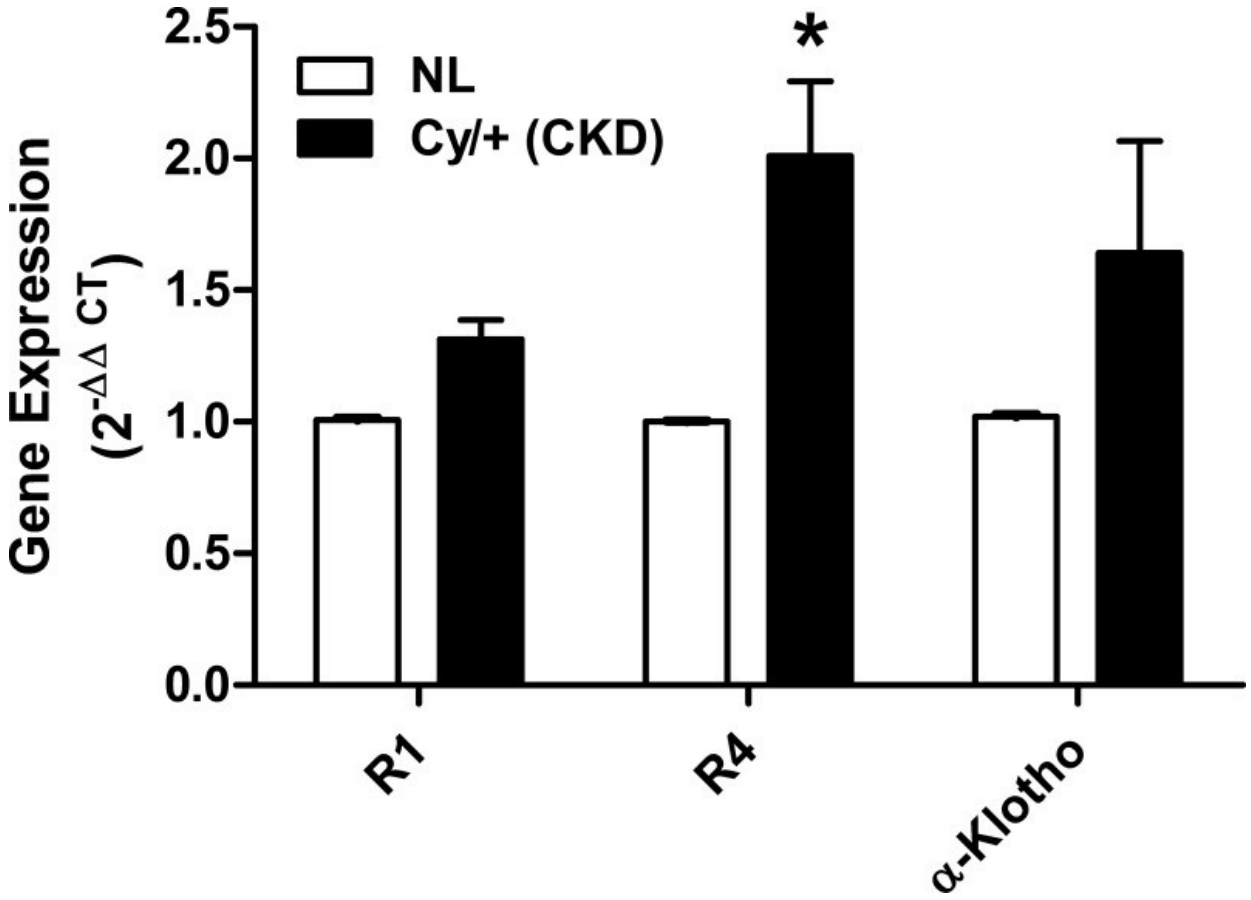

Fgfr4 expression is elevated in the Cy/+ rat model for chronic kidney disease (CKD). Differences in gene expression of *Fgfr1*, *r4*, and *α-Klotho* in EDL muscle from Cy/+ rats or normal littermates (NL) were calculated using the $2^{-\Delta\Delta C_T}$ method ($n = 6$). *$P < 0.05$ vs. NL, 1-way ANOVA with Bonferroni post hoc analysis.

Fig. 3.

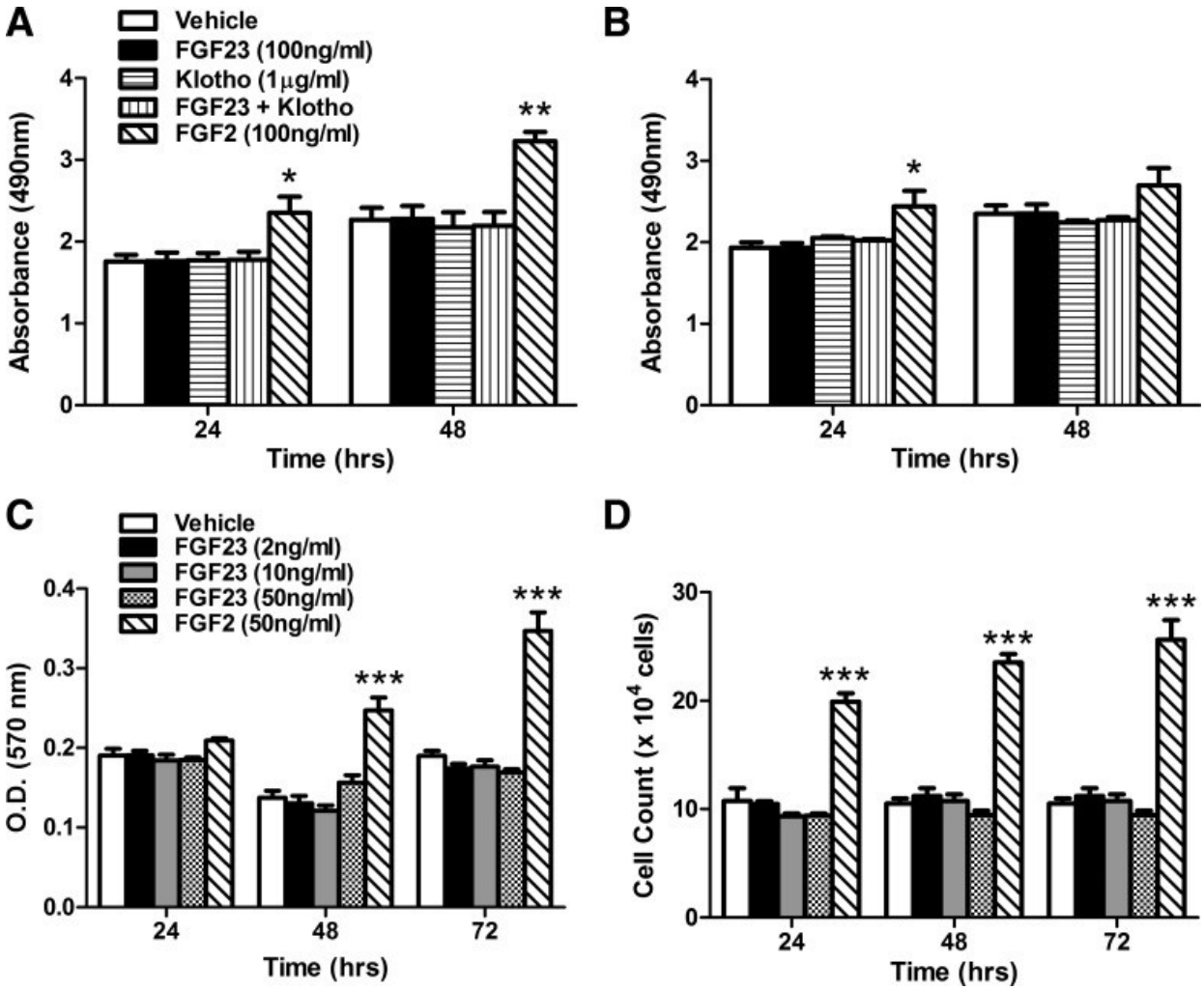

FGF23 treatment has no effect on C_2C_{12} proliferation. *A* and *B*: cellular proliferation of undifferentiated C_2C_{12} myoblasts (*A*) and differentiated C_2C_{12} myotubes (*B*) treated with FGF23 (100 ng/ml), soluble Klotho (1 μg/ml), FGF23 + Klotho, or FGF2 (100 ng/ml, positive control) for 24 and 48 h, as assessed by absorbance at 490 nm using CellTiter 96 AQueous One kit ($n = 3$; 3 separate experiments). *C*: MTT assay of undifferentiated C_2C_{12} myoblast proliferation after treatment with FGF23 (2–50 ng/ml) or FGF2 (50 ng/ml) for 24, 48, and 72 h ($n = 4$; repeated twice). *D*: hemocytometer-based cell count of undifferentiated C_2C_{12} myoblasts after treatment with FGF23 (2–50 ng/ml) or FGF2 (50 ng/ml) for 24, 48, and 72 h ($n = 3$; repeated twice). $^*P < 0.05$, $^{**}P < 0.01$, and $^{***}P < 0.001$, 1-way ANOVA with Bonferroni post hoc analysis.

Fig. 4.

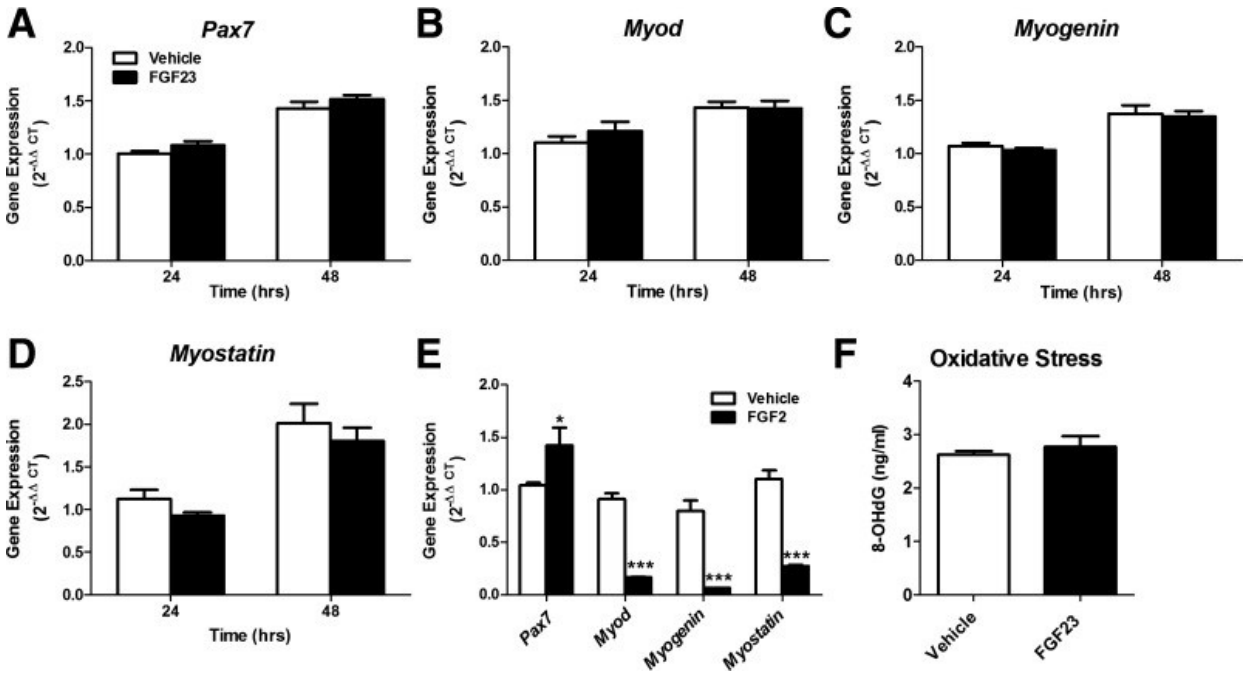

FGF23 treatment does not alter expression of myogenic markers or oxidative stress. *A–D*: expression of myogenic gene markers *Pax7* (*A*), *Myod* (*B*), *Myogenin* (*C*), and *Myostatin* (*D*) in differentiated C_2C_{12} myotubes after treatment with FGF23 (100 ng/ml) or vehicle for 24 and 48 h. Gene expression was calculated using the $2^{-\Delta\Delta C_T}$ method ($n = 6$). *E*: positive control data showing expression of *Pax7*, *Myod*, *Myogenin*, and *Myostatin* in differentiated C_2C_{12} myotubes after treatment with FGF2 (100 ng/ml) or vehicle for 48 h ($n = 3$). *$P < 0.05$ and ***$P < 0.001$, 1-way ANOVA with Bonferroni post hoc analysis. *F*: oxidative stress was assessed by measuring the DNA oxidative damage marker 8-hydroxy-2′-deoxyguanosine (8-OHdG) in differentiated C_2C_{12} myotubes after 24-h treatment with FGF23 (100 ng/ml) or vehicle ($n = 6$). $P > 0.05$, Student's *t*-test.

Fig. 5.

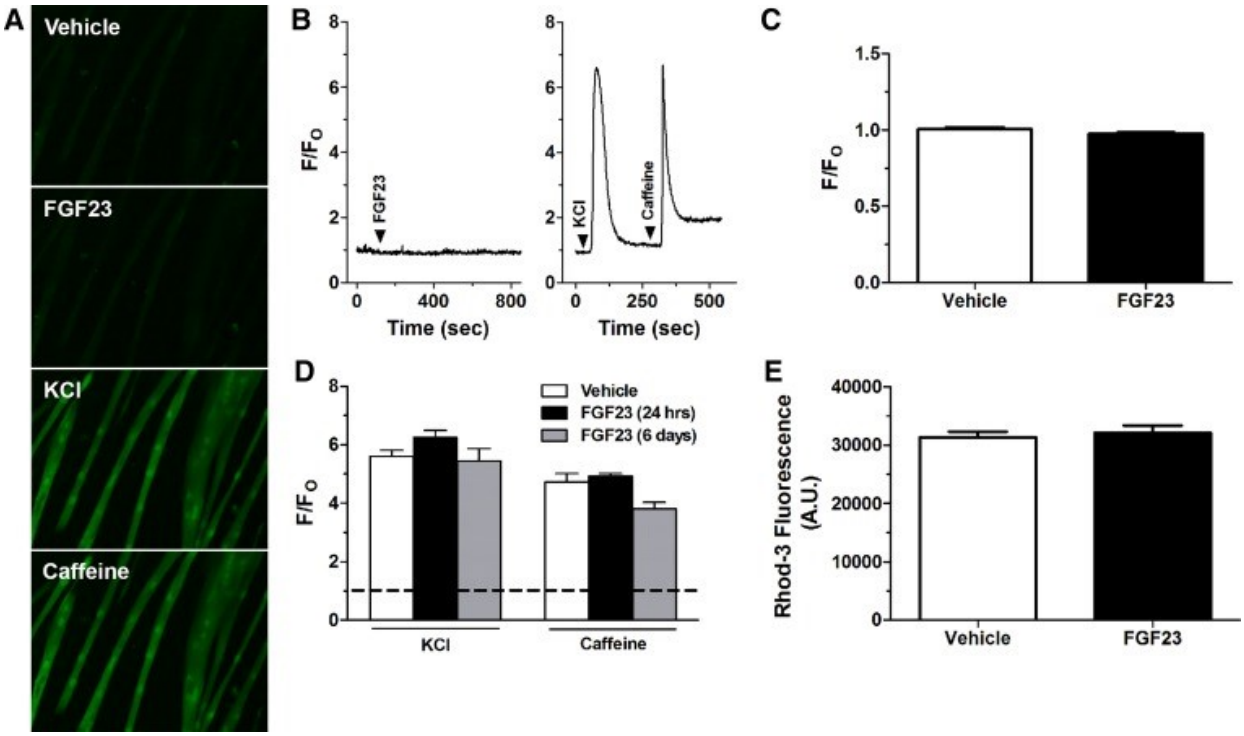

Neither acute nor long-term FGF23 treatment has an effect on C_2C_{12} myotube $[Ca^{2+}]_i$. *A*: representative fluo-4 fluorescent images in C_2C_{12} cells after vehicle, FGF23 (20 ng/ml), KCl (80 mM), or caffeine (20 mM) perfusion. Note the increase in fluorescence after KCl and caffeine treatment but not FGF23. *B*: representative fluo-4 fluorescence signal and perfusion protocol showing acute C_2C_{12} myotube $[Ca^{2+}]_i$ responses to FGF23 (20 ng/ml) (*left*) and KCl (80 mM) and caffeine (20 mM) perfusion (*right*). Arrowheads indicate points of perfusion of specific treatments. The fluorescence signal is expressed relative to baseline (F/F_O). *C*: data summary of average peak change in fluo-4 fluorescence after perfusion with FGF23 (20 ng/ml) or vehicle expressed relative to baseline (F/F_O) ($n = 3$ dishes/group with 7–8 myotubes/dish averaged). $P > 0.05$, Student's *t*-test. *D*: average change in fluo-4 fluorescence in response to perfusion with KCl (80 mM) and caffeine (20 mM) in myotubes incubated with FGF23 (20 ng/ml) for 24 h or 6 days ($n = 3$–6 dishes/group with 5–11 myotubes/dish averaged). Horizontal dashed line indicates the fluorescence level at baseline before stimulation of Ca^{2+} release. $P > 0.05$, 1-way ANOVA. *E*: Rhod-3 fluorescence in differentiated C_2C_{12} myocytes after treatment with FGF23 (100 ng/ml) for 4 h ($n = 6$). $P > 0.05$, Student's *t*-test.

Fig. 6.

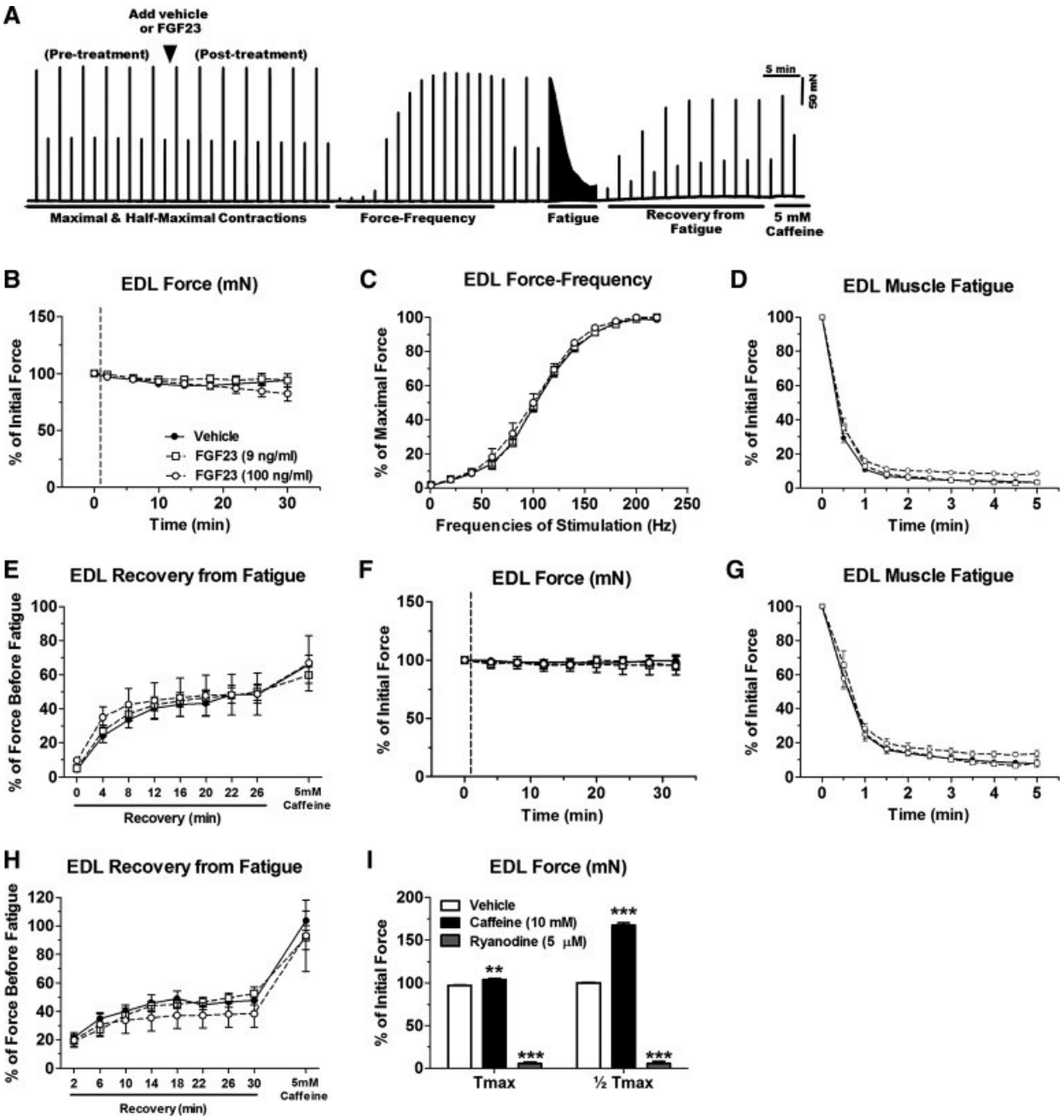

Open in a separate window

Acute FGF23 administration does not alter CD-1 mouse EDL muscle contractile properties. *A*: representative ex vivo contractility force data obtained from 1 muscle (*x*-axis: time; *y*-axis: force) showing an entire contraction protocol and time of FGF23 addition. *B*: maximal tetanic force output (at 200-Hz stimulation) from CD-1 mouse EDL muscles after treatment with vehicle or FGF23 expressed relative to values before vehicle or FGF23 application. *C*: force-frequency relationship of vehicle- or FGF23-treated EDL muscles stimulated to contract with frequencies in the range of 1–220 Hz. Forces at each frequency are expressed relative to the maximal force obtained. *D*: time course of maximal tetanic force decline during a fatiguing protocol in vehicle- or FGF23-treated EDL muscles. Force at each time point is expressed relative to force just before fatigue. *E*: maximal tetanic force recovery during various time points postfatigue and with the addition of 5 mM caffeine in vehicle- or FGF23-treated EDL muscles. *F*: half-maximal tetanic force output (at 100-Hz stimulation) from CD-1 mouse EDL muscles after treatment with vehicle or FGF23 expressed relative to values before vehicle or FGF23 application. *G*: time course of half-maximal tetanic force decline during a fatiguing protocol in vehicle- or FGF23-treated EDL muscles. Force at each time point is expressed relative to force just before fatigue. *H*: half-maximal tetanic force recovery during various time points postfatigue and with the addition of 5 mM caffeine in vehicle- or FGF23-

treated EDL muscles. *I*: maximal and half-maximal tetanic force after exposure of EDL muscles to 10 mM caffeine or 5 μM ryanodine, as positive controls, expressed as %force before vehicle or FGF23 treatment (however, error bars that are present in each group may be too small to be seen). Dashed lines in *B* and *F* represent points at which FGF23 was added to the muscle contractility bath; $n = 3–10$ muscles/group. $^{**}P < 0.01$ and $^{***}P < 0.001$, 2-way ANOVA with Bonferroni post hoc analysis.

Fig. 7.

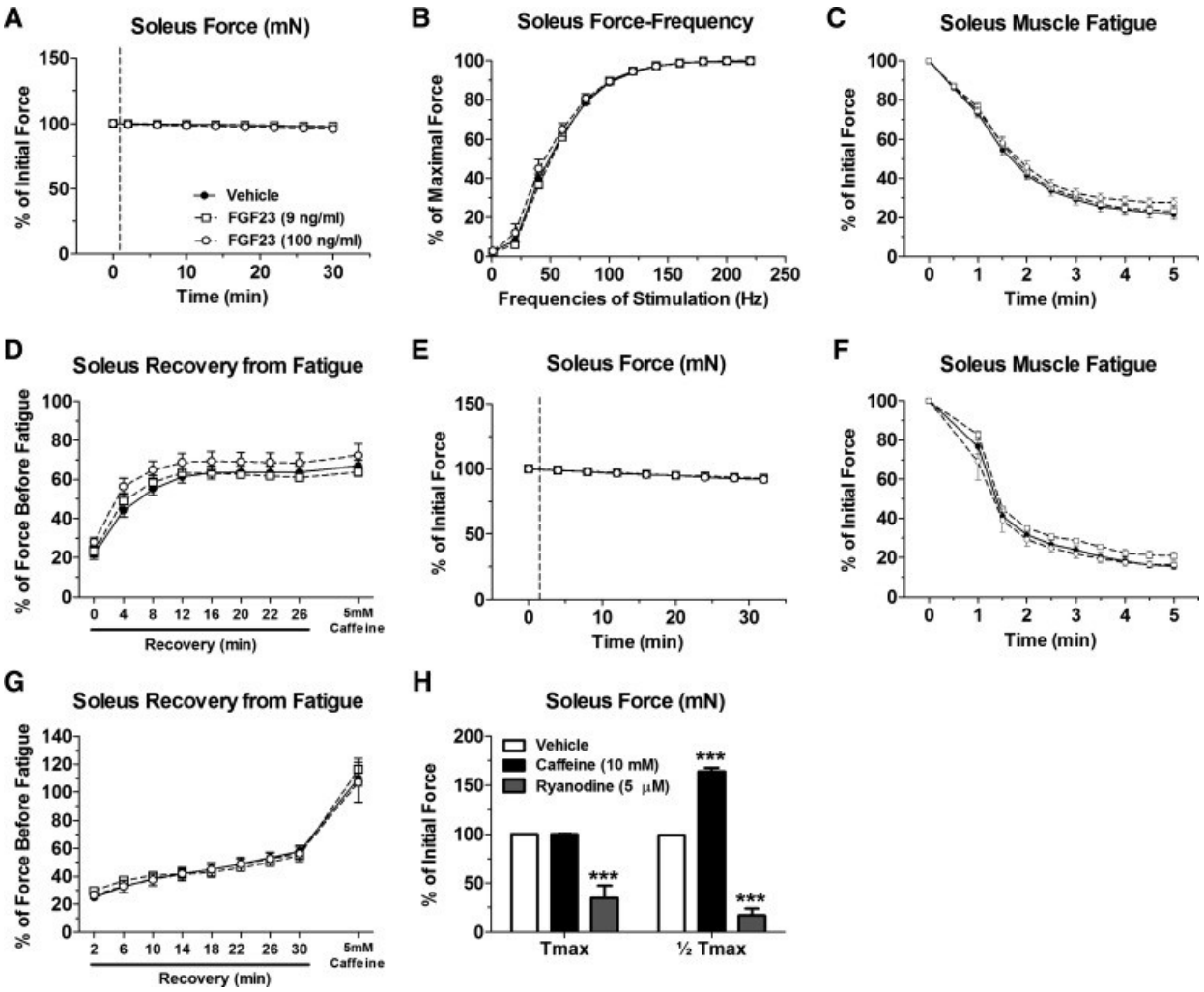

Acute FGF23 administration does not alter CD-1 mouse soleus muscle contractile properties. *A*: maximal tetanic force output (at 140–160 Hz stimulation) from CD-1 mouse soleus muscles after treatment with vehicle or FGF23 expressed relative to values before vehicle or FGF23 application. *B*: force-frequency relationship of vehicle- or FGF23-treated soleus muscles stimulated to contract with frequencies in the range of 1–220 Hz. Forces at each frequency are expressed relative to the maximal force obtained. *C*: time course of maximal tetanic force decline during a fatiguing protocol in vehicle- or FGF23-treated soleus muscles. Force at each time point is expressed relative to force just before fatigue. *D*: maximal tetanic force recovery during various time points postfatigue and with the addition of 5 mM caffeine in vehicle- or FGF23-treated soleus muscles. *E*: half-maximal tetanic force output (at 40 Hz stimulation) after treatment with vehicle or FGF23 expressed relative to values before vehicle or FGF23 application. *F*: time course of half-maximal tetanic force decline during a fatiguing protocol in vehicle- or FGF23-treated soleus muscles. Force at each time point is expressed relative to force just before fatigue. *G*: half-maximal tetanic force recovery during various time points postfatigue and with the addition of 5 mM caffeine in vehicle- or FGF23-treated soleus muscles. *H*: maximal and half-maximal tetanic force after exposure of soleus muscles to 10 mM caffeine or 5 μM ryanodine, as positive controls, expressed as a %force before vehicle or FGF23 treatment (however, error bars that are present in each group may be too small to be seen). Dashed lines in *A* and *E* represent points at which FGF23 was added to the muscle contractility bath; $n = 5–10$ muscles/group. ***$P <$ 0.001, 2way ANOVA with Bonferroni post hoc analysis.

Fig. 8.

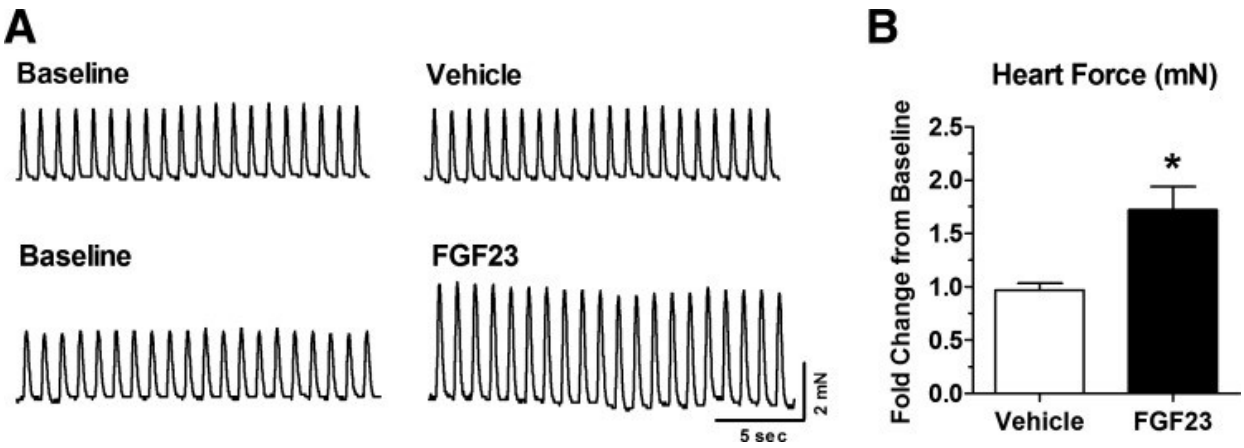

Acute FGF23 administration increases isolated heart contractility. *A*: representative force tracings of isolated mouse heart muscle paced at 1 Hz at baseline (before vehicle or FGF23 treatment) and after 30 min of exposure to vehicle or 9 ng/ml FGF23. *B*: summary data of whole heart contractile force output after 30 min of vehicle or 9 ng/ml FGF23 exposure. Data are expressed as fold change of contractile force relative to baseline; $n = 4–6$ hearts/group. $^*P < 0.05$, 2-tailed *t*-test.